Measurement and Theoretical Study of Electrical Conductivity and Hall Effect in Oxide Cathodes*

R. FORMAN
National Bureau of Standards, Washington, D. C., and University of Maryland, College Park, Maryland
(Received August 23, 1954)

Hall effect and electrical conductivity measurements have been made on the oxide cathode over the temperature range 500° to 1000°K. The Hall coefficient of the oxide cathode is negative and the Hall coefficient has a maximum value in the range 600° to 800°K. Above 700°K the values for electron mobility are very large, and below 700°K the mobility decreases rapidly with decreasing temperature. Large magnetoresistive effects were observed, and these were found to be dependent on the temperature and the degree of porosity of the cathode. These results are consistent with the porous semiconductor model for the oxide cathode as originally suggested by Loosjes and Vink. A mathematical theory, based on the high-temperature pore conductivity model, is developed which is in qualitative agreement with the data.

I. INTRODUCTION

IN recent years two theories have been proposed to explain the physical properties of the oxide cathode. The semiconductor model has been proposed by numerous investigators.[1,2] The other theory, suggested by Loosjes and Vink,[3] states that the oxide cathode is a porous semiconductor in which the following two distinct conduction mechanisms operate in parallel. In the low-temperature regions (below 700°K) the conductivity is predominantly due to semiconduction through the crystals of the coating. In the high-temperature range the conductivity is attributed to an electron gas in the pores of the cathode coating. Recently additional evidence has been reported indicating that the Loosjes and Vink theory may be valid,[4–6] but the evidence is far from conclusive.[2,7]

Hall and conductivity measurements offer a means for differentiating between the two physical models. Such measurements,[7–9] at temperatures above 700°K, have been reported in the literature. The results have been interpreted, by using a semiconductor model, but a number of anomalous observations were reported which seem inconsistent with this model, such as (1) large Hall coefficients, (2) high values for the mobility, and (3) large magnetoresistive effects.

In the following sections, measurements of conductivity and Hall effect of oxide cathodes over the temperature range 500° to 1000°K are described. A mathematical theory is then developed, based on the model suggested by Loosjes and Vink, which explains the experimental data at elevated temperatures and is consistent with data obtained by previous investigators. The theory is then compared with the experimental data, and the results are interpreted.

II. EXPERIMENTAL PROCEDURE

A magnesium oxide crucible, shown in Fig. 1, was used as the sample holder. The crucibles were prepared from MgO of 99.8 percent purity, shown as *C*, and a description of their preparation is given elsewhere.[10]

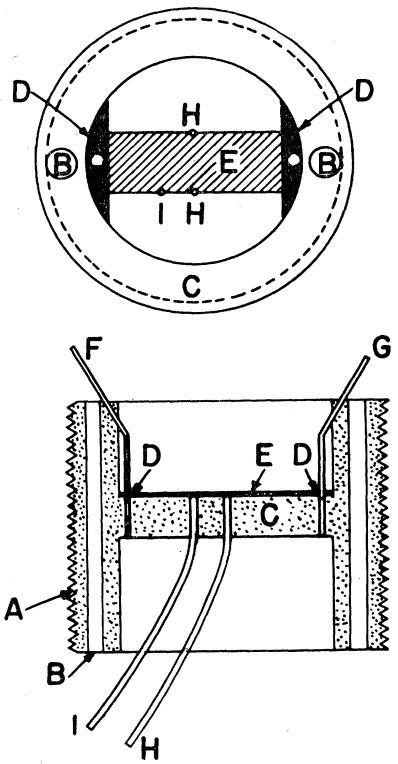

FIG. 1. MgO base used as a sample holder for the deposited oxide cathode. *A* designates a bifilar winding on the MgO base and *B* denotes the support holes. The lead *G* is also the platinum part of a Pt-Pt (13 percent Rh) thermocouple.

* This paper is a portion of a dissertation presented by the author in partial fulfillment of the requirements for the degree of Doctor of Philosophy at the University of Maryland.

[1] Hannay, McNair, and White, J. Appl. Phys. **20**, 669 (1949).
[2] L. S. Nergaard, R.C.A. Rev. **13**, 464 (1952).
[3] R. Loosjes and H. J. Vink, Philips Research Repts. **4**, 449 (1949).
[4] R. C. Hughes and P. P. Coppola, Phys. Rev. **88**, 364 (1952).
[5] E. B. Hensley, J. Appl. Phys. **23**, 1122 (1952).
[6] J. R. Young, J. Appl. Phys. **23**, 1129 (1952).
[7] D. A. Wright and J. Wood, Proc. Roy. Soc. (London) **65B**, 134 (1952).
[8] D. A. Wright, Brit. J. Appl. Phys. **1**, 150 (1950).
[9] Ishikawa, Sato, Okumura, and Sasaki, Phys. Rev. **84**, 371 (1951).
[10] W. B. Haliday and J. R. Nall, Rev. Sci. Instr. **25**, 1225 (1954).

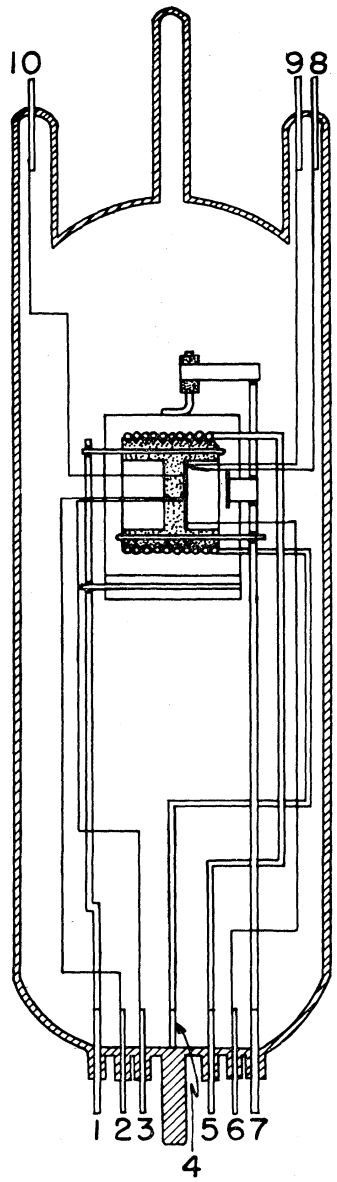

FIG. 2. Vacuum tube for making Hall and conductivity measurements on the oxide cathode.

The metal-ceramic patches D were prepared by a technique similar to the Telefunken process developed for metal-ceramic brazes. The metallic contacts D make electrical contact to the oxide coating E and also serve to bind the lead F and the lead G in place as electrical leads to the sample. The probe wires H and I were fixed firmly in place by drilling holes in the crucible while it was in the unfired state. Platinum probes having the same diameter (0.015 in.) as the holes were then inserted, and the crucible was fired to 1650°C in air. During the firing the ceramic shrank 9 to 12 percent, and the platinum leads became firmly imbedded. The cathode coating is a double carbonate known commercially as C51-2 and is prepared from an equimolecular mixture of barium and strontium carbonates. The cathodes were sprayed with a type CV-DeVilbiss spray gun. Each of the various coatings was approximately one cm in length, 0.25 cm wide and 0.01 cm thick.

A platinum heater wire was wound over the bifilar threaded portion of the crucible which was then mounted in a tube sketched in Fig. 2. A molybdenum anode for collecting emission current and a molybdenum heat shield are incorporated in the tube. The anode lead also supports the heat shield but is insulated from it by an alundum sleeve. The tube contained a batalum getter which was welded to one of the leads in the tube.

The tube was processed on a vacuum system which included an oil diffusion pump, two Westinghouse metal valves, thermocouple and ionization gauges, and an ethane gas bottle. The high-vacuum end of the system was baked out at 400°C for 14 hours, and the metal parts in the tube were outgassed by inductive heating before the cathodes were processed. Activation consisted of treating the cathodes in ethane using a procedure similar to that described by Wright.[8] In general, as a result of activation, both emission and conductivity increased by a factor of 10–20. The pressure in the tubes, before they were sealed off the vacuum system, was better than 10^{-6} mm of Hg.

Five tubes were prepared and tested, and they are designated in the text as CH3 to CH7 inclusively. The density[11] or porosity of the cathodes in these five tubes were varied. Table I describes the properties of the different cathodes.

Measurement difficulties were experienced with tube CH3. The Hall and conductivity probes in this tube extended above the sample, making very poor contact with the oxide coating, and this was responsible for generating noise voltages at low temperatures. This difficulty was eliminated in all of the other tubes by cutting the probes down flush with the MgO base and then depositing the coating over the probes so that they were completely covered by the sample.

Preliminary experiments on the conductivity of the oxide cathode indicated that the resistance of some samples was as high as 10^{10} ohms at low temperatures (500°K). Such high-resistance samples required the use of a vibrating reed electrometer, such as that of the Applied Physics Laboratory of Pasadena, California,

TABLE I. Properties of the different cathodes.

Tube	Density of coating g/cm³	Method of depositing coating	Activated with ethane
CH3	0.3–0.4	Sprayed	No
CH4	0.7–0.8	Sprayed	Yes
CH5	0.9–1.0	Sprayed	No
CH6	0.4–0.5	Sprayed	Yes
CH7	1.3–1.4	Brushed on	Yes

[11] The density was measured by depositing the oxide alternately on the magnesia base and on a nickel strip in an identical manner. The weight and dimensions of the coating were then measured on the nickel strip.

as a voltage-indicating device. The electrometer has an input resistance greater than 10^{15} ohms and will not affect the electrical properties of the sample when placed across the Hall or conductivity probes.

The electrical circuit for making these measurements is illustrated in Fig. 3. The switch in the electrometer circuit is a Teflon selector switch. The resistance selector switch is a Centralab ceramic series switch which was coated with polystyrene to reduce leakage as described by Glass.[12] The reversing switches and batteries, which supply the conduction current through the sample, are encased in a polystyrene box to insulate them from the shielded box enclosing the electrical circuit. The 1.5-volt cell in the Hall circuit is used to eliminate the IR drop across the Hall probes. The current through the sample is determined by the voltage drop across the fixed resistors R_1, R_2, R_3, and R_4. Their respective values are 10^5, 10^6, 10^7, and 10^9 ohms. To minimize thermionic electron currents when Hall and conductivity measurements were made, it was necessary to bias the heater positive with respect to the heat shield and the sample positive with respect to the molybdenum anode. Extreme shielding precautions had to be taken in these measurements in order to obtain reliable results.

The conductivity and Hall measurements were made by the following procedure. After the tube was placed between the magnet pole faces, with the magnetic field direction perpendicular to the sample face, the temperature of the sample was raised to the highest value it attained in the measurements. The temperature of the cathode was recorded after it reached thermal equilibrium. The current through the sample was regulated to give the most advantageous voltage reading. This could be accomplished in practically all cases by the use of the 1.5-volt battery source. The voltage drop across the conductivity probes and the current through the sample were then measured with no applied magnetic field. In general, when the magnetic field was applied, the current through the sample changed markedly due to the high magnetization resistance of the material. The value of the current through the sample with an applied magnetic field was recorded and checked by reversing the polarity of the magnetic field. The Hall voltage was then measured with the magnetic field in a given direction and then of opposite polarity. The field strength used in practically all Hall measurements was either 500 or 1000 gauss. The temperature of the sample was then progressively lowered approximately 50°C at a time, and similar electrical data taken at each setting. The lowest temperature at which measurements could be taken was limited by (a) the Hall voltages becoming indetectable or (b) noise fluctuations across the high-resistivity samples becoming appreciable. A few points were also taken on a reheating cycle to insure the reproduceability of the data.

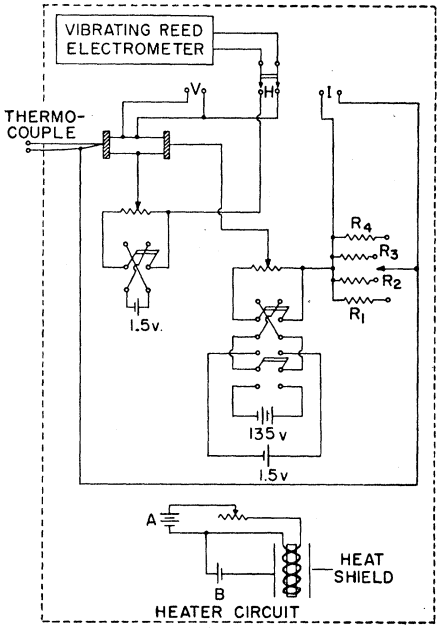

FIG. 3. Circuit diagram of electrical equipment for measuring the conductivity and the Hall coefficient at different temperatures.

[12] F. M. Glass, Rev. Sci. Instr. **20**, 239 (1949).

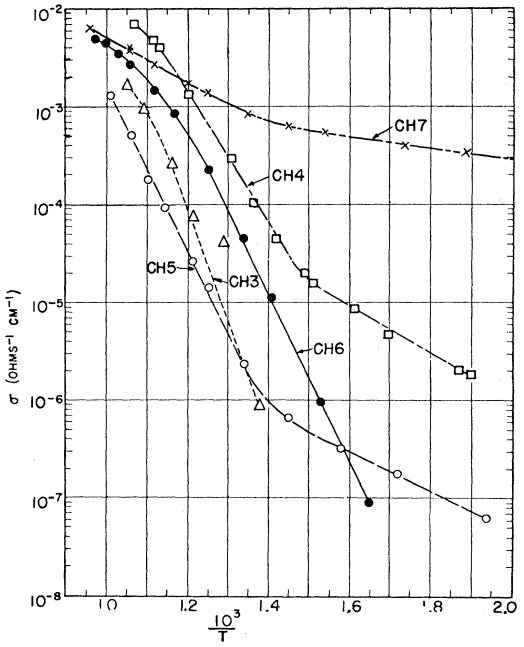

FIG. 4. Conductivity of the oxide cathode as a function of the inverse absolute temperature. Properties of the different cathodes are shown in Table I.

III. EXPERIMENTAL RESULTS

Conductivity and Hall data for the five tubes tested are shown in Figs. 4 and 5. The relative porosities of the different cathodes are shown in Table I.

The denser cathodes illustrate the break in the slope of the conductivity curve at about 700°K as described

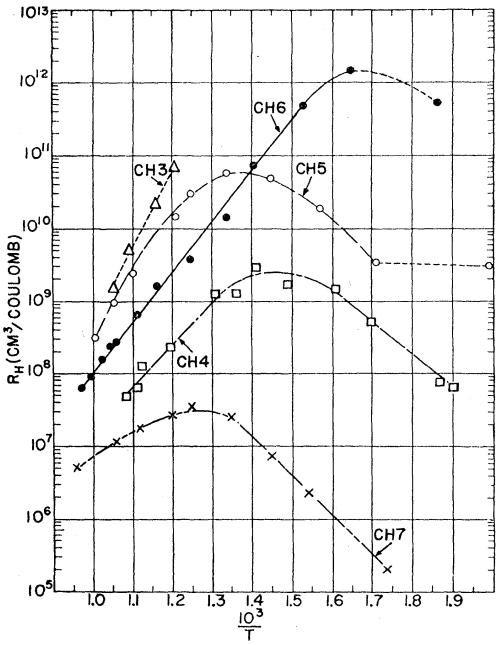

FIG. 5. Hall coefficient of the oxide cathode as a function of the inverse absolute temperature. Properties of the different cathodes are shown in Table I. The last point in the Hall curves for CH5 and CH6 are upper limits for the Hall coefficient. The accuracy of the measurements in these two tubes was limited by noise and is indicated in both curves by the dashed portion.

by Loosjes and Vink.[3] This is seen to be independent of activation. In the temperature range covered by these measurements, the most porous cathodes do not show any break in the slope of the conductivity curve. The magnitude of the Hall coefficient was relatively large and the sign of the Hall coefficient was negative on all samples. Figure 5 shows that all the Hall curves, except that for CH3, have a maximum. Data on CH3 at lower temperatures were not taken because of the higher noise level in the tube. Experimental evidence was obtained which showed that the Hall coefficient was independent of magnetic field at high temperatures and dependent on magnetic field at lower temperatures, corresponding to the transition temperature range discussed later, but this was not investigated in great detail.

If the Hall coefficient or conductivity curves are considered as exponential functions of T for all samples, one finds that the activation energies, as determined from the slopes of the linear portions of the curves at high temperatures, fall within the range of 0.5 to 2.2 ev. For a given sample the values of the activation energy in the high temperature range, obtained from the conductivity and Hall curves respectively, differ by not more than 0.25 ev.

TABLE II. Apparent mobility of different cathodes at 1000°K.

Tube No.	CH3	CH4	CH5	CH6	CH7
Mobility (cm^2/volt sec)	4×10^6	3×10^5	4×10^5	4×10^5	3×10

An "apparent" mobility of the carriers, μ, in all these samples is defined by the usual relation, $\mu=\sigma_0 R_H$, where σ_0 is the conductivity with no applied magnetic field and R_H is the Hall coefficient.[13] The mobility at high temperatures, 800° to 1000°K, was found to be large for all samples. As the temperature was progressively lowered, the "apparent" mobility decreased with decreasing temperature. The values for mobility of the different samples at approximately 1000°K are tabulated in Table II. The data on tubes CH4, CH5, CH6, and CH7 are considered to be more reliable than those for CH3, because of the difficulty with the probe wires of the latter tube mentioned earlier.

The oxide cathode also exhibits very unusual conductivity properties in the presence of a magnetic field. The resistivity of some of the samples could be increased by a factor of ten by applying a transverse magnetic field of 500 gauss. The marked change in conductivity is illustrated in Fig. 6 which is a plot of the fractional change in conductivity with applied magnetic field for the tubes CH4, CH5, CH6, and CH7.

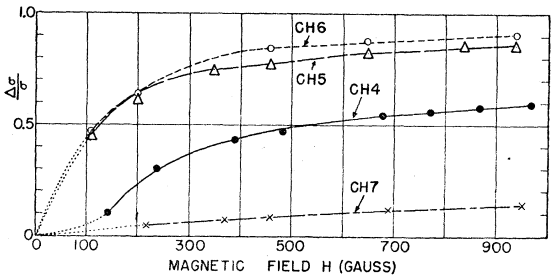

FIG. 6. Fractional change in conductivity with increasing magnetic field for the oxide cathode. Properties of the different cathodes are shown in Table I. CH6 is the most porous sample and CH7 is the least porous.

The data on all tubes were taken at approximately the same temperature, 950°K. Similar behavior has been observed previously.[9]

IV. THEORY

The experimental data of the previous section are inconsistent with the theory developed for the oxide cathode as a semiconductor. In order to explain the large values of Hall coefficient and mobility at high temperatures, a maximum at high temperatures in the curve of $\log R_H$ *vs* T^{-1}, and a large variation of resistance with magnetic field, a theory, based on the pore conduction hypothesis of Loosjes and Vink, will be proposed as a basis for interpreting the experimental results.

The proposed theoretical model assumes that the oxide cathode contains irregularly shaped channels, composed of irregularly shaped pores or cavities, whose

[13] This definition loses its significance when several mechanisms of conduction arise. Such a situation will be discussed later.

walls are thermionic emitters. The mean free path in this channel is assumed to be dependent only on the geometry and linear dimensions of the pores. At high temperatures, an electron gas, in thermodynamic equilibrium, will then exist in the channel, and the electric and magnetic properties of this gas will be studied. The model assumes that the conduction mechanism in the oxide cathode at high temperatures is predominantly due to a flow of electrons through the pores and that conduction current through the pore walls is negligible.

A simple kinetic theory treatment of the electron gas indicates that the mobility, μ, is given by the expression[14]

$$\mu=\frac{el}{2(3km)^{\frac{1}{2}}}T^{-\frac{1}{2}}, \tag{1}$$

where l is the mean free path or linear dimension of the pore, and e, m, k, and T are the electronic charge, electronic mass, Boltzmann's constant, and the temperature, respectively. A more general treatment, however, is desirable. This treatment is similar to that developed by Gans[15] for the free electron theory of metals and is in Seitz.[16]

The electron gas is assumed to obey Maxwell-Boltzmann statistics and the distribution function, f_0, giving the number of particles in a volume element $dxdydzdv_xdv_ydv_z$ in phase space, is given by

$$f_0=\frac{2m^3}{h^3}\exp\left\{-\frac{e\phi}{kT}\right\}\exp\left\{-\frac{\epsilon-eV_p(x,y,z)}{kT}\right\}. \tag{2}$$

ϕ is the work function for the material in the emitting walls, ϵ is the kinetic energy, and $V_p(x,y,z)$ is the electrostatic potential energy for the electrons in the volume element in phase space. The quantities m, k, and h are respectively the electronic mass, Boltzmann's constant, and Planck's constant. In this treatment it is assumed that the mean free path for the electrons is determined by the average linear dimensions l of the pores.

If a crossed electric and magnetic field is applied (i.e., electric field in the x direction, magnetic field in the z direction), the new distribution function, f, is given to a first approximation by

$$f=f_0+v_x\chi_1(v)+v_y\chi_2(v), \tag{3}$$

where χ_1 and χ_2 are functions of the scalar magnitude of $\mathbf{v}$; v_x and v_y are the respective electron velocities in the x and y directions. Assuming that the collisions between the electron gas and cavity walls are elastic[17] and isotropic and that no temperature gradient exists, one finds, following the method of reference 15, that the conductivity, σ_H, and the isothermal Hall coefficient, R_H, are given by

$$\sigma_H=\frac{I_x}{E_x}=-\frac{4\pi e^2}{3}\frac{L_1^2+L_2^2}{L_1}, \tag{4}$$

$$R_H=\frac{E_yc}{I_xH_z}=\frac{3}{4\pi e^2}\frac{L_2}{L_1^2+L_2^2}\frac{c}{H_z}, \tag{5}$$

where

$$L_1=\int_0^\infty\frac{lv^2}{1+s^2}\frac{\partial f_0}{\partial\epsilon}vdv, \tag{6}$$

$$L_2=\int_0^\infty\frac{lsv^2}{1+s^2}\frac{\partial f_0}{\partial\epsilon}vdv, \tag{7}$$

and

$$s=elH_z/mcv. \tag{8}$$

When L_1 and L_2 are evaluated, using the distribution function f_0 [Eq. (2)], the expressions for σ_H and R_H become

$$\sigma_H=\frac{16\pi e^2ml}{3h^3}kT\exp\left\{-\frac{e(\phi-\bar{V}_p)}{kT}\right\}\frac{F_1^2+F_2^2}{F_1}, \tag{9}$$

and

$$R_H=-\frac{3ch^3}{16\pi e^2mlkTH_z}\exp\left\{\frac{e(\phi-\bar{V}_p)}{kT}\right\}\frac{F_2}{F_1^2+F_2^2}; \tag{10}$$

where

$$F_1\left(\frac{a}{kT}\right)=1-\left(\frac{a}{kT}\right)+\left(\frac{a}{kT}\right)^2\times\exp\left\{\frac{a}{kT}\right\}\left[-\mathrm{Ei}\left(-\frac{a}{kT}\right)\right], \tag{11}$$

$$F_2\left(\frac{a}{kT}\right)=\left(\frac{a}{kT}\right)^{\frac{1}{2}}\left[\frac{\pi^{\frac{1}{2}}}{2}-\pi^{\frac{1}{2}}\left(\frac{a}{kT}\right)+\pi\left(\frac{a}{kT}\right)^{\frac{3}{2}}\times\exp\left(\frac{a}{kT}\right)\mathrm{erfc}\left\{\left(\frac{a}{kT}\right)^{\frac{1}{2}}\right\}\right], \tag{12}$$

$$a=e^2l^2H_z^2/2mc^2, \tag{13}$$

and $\bar{V}_p$ is the average electrostatic potential energy in the cavity. The functions F_1, F_2, and $F_1^2+F_2^2$ are plotted graphically in Fig. 7.

The conductivity, σ_0, of the electron gas model, with no applied magnetic field, is given by setting $F_1=1$ and $F_2=0$ in Eqs. (11) and (12). The result is

$$\sigma_0=\frac{16\pi e^2ml}{3h^3}kT\exp\left\{-\frac{e(\phi-\bar{V}_p)}{kT}\right\} \tag{14}$$

which is very similar to the expression derived by Hensley[5] by a different approach using a similar model.

The mobility obtained from the experimental data by the usual relationship, $\mu=\sigma_0R_H$, can be theoretically

[14] All derivations in this paper are in Gaussian units.
[15] R. Gans, Ann. Physik **20**, 293 (1906).
[16] F. Seitz, *The Modern Theory of Solids* (McGraw-Hill Book Company, Inc., New York and London, 1940), pp. 168–194.
[17] This simple assumption may be too idealized, but it leads to results which are of the correct order of magnitude.

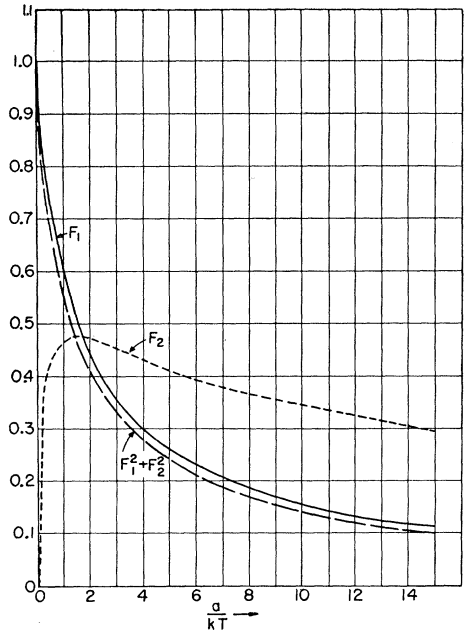

FIG. 7. The numerical values of the functions F_1, F_2 [Eqs. (11) and (12)] and $F_1^2+F_2^2$ plotted as a function of the parameter a/kT. The abscissa a/kT is equal to $e^2l^2H_z^2/2mc^2kT$. For a given mean free path and temperature the abscissa is proportional to the value of the magnetic field squared.

determined from Eqs. (10) and (14). This is given by

$$\sigma_0 R_H=\frac{el}{(2mk)^{\frac{1}{2}}}T^{-\frac{1}{2}}\left(\frac{a}{kT}\right)^{-\frac{1}{2}}\frac{F_2}{F_1^2+F_2^2}. \tag{15}$$

It can be shown that the order of magnitude of $\{(a/kT)^{-\frac{1}{2}}F_2/F_1^2+F_2^2\}$ is approximately unity for all values of a/kT, and this leads to the expression

$$\mu=\sigma_0 R_H\cong\frac{el}{(2mk)^{\frac{1}{2}}}T^{-\frac{1}{2}}. \tag{16}$$

If the theoretical expression for the density of electrons is computed, the result is given by

$$n=\int_{-\infty}^{\infty}\int_{-\infty}^{\infty}\int_{-\infty}^{\infty}f_0 dv_x dv_y dv_z$$
$$=\frac{2}{h^3}(2\pi mkT)^{\frac{3}{2}}\exp\left\{-\frac{e(\phi-\bar{V}_p)}{kT}\right\}. \tag{17}$$

From Eqs. (10) and (17) and the same approximation as above for $\{(a/kT)^{-\frac{1}{2}}F_2/F_1^2+F_2^2\}$, an expression can be derived relating the Hall coefficient to the density of carriers, namely,

$$R_H\cong-1/en, \tag{18}$$

which is very similar to the functional relationship of these quantities in semiconductor theory.

Another quantity which is of considerable interest, theoretically and experimentally, is that of the fractional change of conductivity with applied magnetic field. From Eqs. (9) and (14) this is given by

$$\Delta\sigma/\sigma_0=1-(\sigma_H/\sigma_0)=1-F_1-F_2^2/F_1. \tag{19}$$

If $\Delta\sigma/\sigma_0$ is plotted as a function of a/kT (H_z is the variable parameter in a/kT), the maximum fractional change in conductivity is given by

$$\lim_{a/kT\to\infty}\frac{\Delta\sigma}{\sigma_0}\to 0.116. \tag{20}$$

This value is low compared to what one observes in the experimental data. The above theory gives order-of-magnitude agreement with the experimental mobility data, but Eq. (20) shows that the theory does not give satisfactory results if effects smaller than an order of magnitude are considered.

An expression, which is consistent with the experimental data for magnetoresistive effects, can be obtained by a modification of the previous treatment. If an electron follows a cyclic or trochoidal path in a crossed electric and magnetic field, it obtains a steady drift velocity in a direction perpendicular to both the electric and magnetic fields. Since the drift is at right angles to the electric field, the cyclic electrons on the average do not contribute to the conduction current. This leads to the hypothesis that only those electrons which suffer collisions in a time short compared to the period of the cycloidal motion contribute to the conduction current. This hypothesis can be incorporated into the theory if it is assumed that only those electrons whose x component of velocity is greater than $v_{0x}=elH_z/mc$, where eH_z/mc is the cyclotron frequency, contribute to the conduction current. One then obtains for the current in the x direction

$$I_x=-2\int_{v_{0x}}^{\infty}\int_{-\infty}^{\infty}\int_{-\infty}^{\infty}ev_x^2\chi_1(v)dv_x dv_y dv_z, \tag{21}$$

where χ_1 is defined in Eq. (3) and can be evaluated to give

$$\chi_1=-\frac{el}{v}\frac{\partial f_0}{\partial\epsilon}\left[\frac{E_x-sE_y}{1+s^2}\right], \tag{22}$$

where s is given by Eq. (8).

Since the Hall voltage is always smaller than the conduction voltage ($E_x>E_y$) and, in the range of the integration variable, $s<1$, the bracketed term in Eq. (22) becomes E_x. If this simplified expression for χ_1 is inserted in Eq. (21) and the integrand is evaluated, one obtains for the conductivity

$$\sigma_H=A\left[\frac{a}{kT}\left\{i\,\mathrm{erfc}\left(\frac{a}{kT}\right)^{\frac{1}{2}}\right\}+\frac{2a}{kT}\left\{i^2\,\mathrm{erfc}\left(\frac{a}{kT}\right)^{\frac{1}{2}}\right\}\right.$$
$$\left.+2\left\{i^3\,\mathrm{erfc}\left(\frac{a}{kT}\right)^{\frac{1}{2}}\right\}\right], \tag{23}$$

where

$$A=\frac{2^7\pi^{\frac{3}{2}}e^2mlkT}{h^3}\exp\left\{-\frac{e(\phi-\bar{V}_p)}{kT}\right\}, \quad (24)$$

where a is defined in Eq. (13) and

$$\left\{i^n\operatorname{erfc}\left(\frac{a}{kT}\right)^{\frac{1}{2}}\right\}=\int_{(a/kT)^{\frac{1}{2}}}^{\infty}\{i^{n-1}\operatorname{erfc}\xi\}d\xi, \quad n=1, 2\cdots. \quad (25)$$

The notation of Eq. (25) is adopted from Carslaw and Jaeger.[18]

To obtain σ_0 set $H_z=0$ (or $a/kT=0$). The resulting expression is

$$\sigma_0=\frac{2^7\pi^{\frac{3}{2}}e^2mlkT}{h^3}\exp\left\{-\frac{e(\phi-\bar{V}_p)}{kT}\right\}[2\{i^3\operatorname{erfc}(0)\}]. \quad (26)$$

The quantity of particular interest is the fractional change of conductivity with applied magnetic field or the expression $\Delta\sigma/\sigma_0$. This expression has been evaluated numerically from Eqs. (23) and (26) and is shown graphically in Fig. 8. The curve in Fig. 8 is similar to the experimental curves of magnetization conductivity. A comparison of the theory and the experimental data will be made in Sec. V.

V. COMPARISON OF THEORY WITH EXPERIMENT AND CONCLUSIONS

The large values of "apparent" mobility, obtained experimentally, are consistent with the theoretical values for mobility as given by Eqs. (1) and (16). If the mobility is expressed in conventional units, cm²/volt sec, and evaluated at 1000°K, both equations yield a value for mobility given by

$$\mu\cong 10^8 l, \quad (27)$$

where l, the mean free path, is expressed in cm. For a mean free path between 10^{-4} and 10^{-3} cm, this value for mobility is in the same order of magnitude as the experimental values for tubes CH4, CH5, CH6, and CH7 (Table II). This range of values for the mean free path is consistent with the range of values one encounters for the linear dimensions of the pores in an oxide cathode.

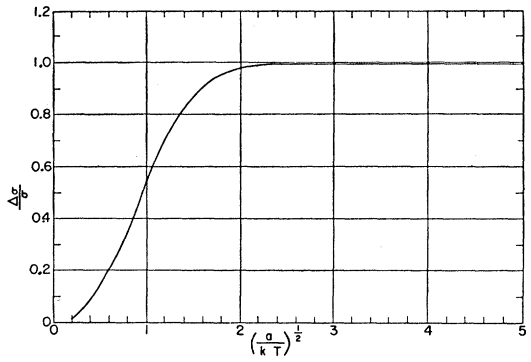

FIG. 8. Theoretical curve of fractional change in conductivity with magnetic field for a constant value of the mean free path and temperature. The abscissa $(a/kT)^{\frac{1}{2}}$ is equal to $elH_z/(2mc^2kT)^{\frac{1}{2}}$ and is proportional to the magnetic field for a given value of l and T.

[18] H. S. Carslaw and J. C. Jaeger, *Conduction of Heat in Solids* (Oxford University Press, London, 1950), p. 371.

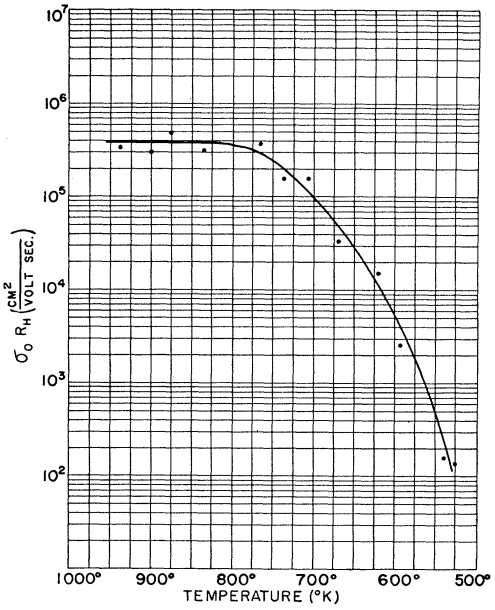

FIG. 9. "Apparent" mobility of sample CH4 *versus* temperature.

Figure 9 illustrates a typical plot of "apparent" mobility, $\mu=\sigma_0R_H$, *vs* temperature. This curve was obtained from sample CH4. These data strongly suggest the validity of the hypothesis originally proposed by Loosjes and Vink. Above 750°K the mobility is high and is consistent with the theoretical value for mobility obtained from the electron gas model. Below 750°K the "apparent" mobility drops rapidly and is approximately 100 cm²/volt sec at 525°K. This low value for mobility is approaching the value one would expect for a semiconductor model. Pell's[19] data on single crystals of barium oxide showed a mobility in the range of 1–10 cm²/volt sec at 500°–800°K. It should be noted that there is theoretical justification for considering σ_0R_H as a mobility at low temperatures (semiconductor) and at high temperatures (electron-gas model), but there is no such justification in the transition region where σ_0R_H is rapidly decreasing and two parallel conduction mechanisms exist.

This leads to the following proposed model for an oxide cathode over the temperature range 500° to 1000°K. At high temperatures (above 700° to 800°K) the mechanism for electrical conduction is predominantly pore conduction. At low temperatures (500°–700°K) there is a transition range where two equivalent parallel mechanisms exist, namely that of pore conduc-

[19] E. M. Pell, Phys. Rev. **87**, 457 (1952).

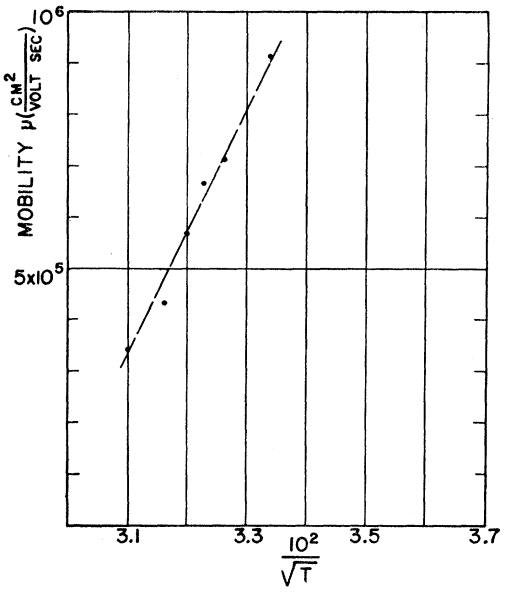

FIG. 10. Plot of mobility of sample CH6 *versus* the inverse of the square root of the absolute temperature.

tion and semiconduction. At the lowest temperature (500°K), semiconduction predominates.

The hypothetical model for the oxide cathode also indicates an explanation for the maximum in the Hall curves of Fig. 5. In the high-temperature range the Hall coefficient increases with decreasing temperature because the density of the electron gas in the pores decreases [Eq. (18)]. As the transition region is reached, the mechanism for semiconduction becomes more important. The density of carriers in the semiconductor is high, and as the temperature is progressively lowered the Hall coefficient decreases, indicating that the density of carriers is increasing as the mechanism of semiconduction takes over.

A break in the conductivity curve like that shown by samples CH4, CH5, and CH7 has been observed previously by other investigators,[3–5] and has been explained by a model similar to that proposed in this paper. The absence of a break in the conductivity curve for CH6 can be attributed to the fact that the area of contact between crystalline particles is probably small because CH6 had a high degree of porosity. This is also consistent with the Hall data for CH6, which has a maximum below the temperature range in which the conductivity was measured.

Another interesting comparison can be made between the experimental data and the theory if one considers the variation of mobility with temperature in the high-temperature region. Equation (16) predicts the mobility is proportional to $T^{-\frac{1}{2}}$. This relationship has been found in samples CH3 and CH6. The data for CH6 is plotted in Fig. 10 and is seen to be in agreement with the theory. The denser samples CH4, CH5, and CH7 did not illustrate this behavior. The mobility data at high temperatures for these samples were scattered as illustrated in Fig. 9 for CH4.

A comparison between the theory and experiment can also be made on the fractional change of conductivity with magnetic field. The abscissa coordinate in Fig. 8 is given as

$$\left(\frac{a}{kT}\right)^{\frac{1}{2}}=\frac{el}{(2mc^2kT)^{\frac{1}{2}}}H_z. \tag{28}$$

If one assumes $l\cong 10^{-3}$ cm and $T=950$°K, then $(a/kT)^{\frac{1}{2}}\cong 10^{-3}H_z$. This theoretically predicts a saturation effect in the magnetization conductivity at about 2000 gauss. This differs by a factor of 2 or 3 with the data from the experimental curves for CH4, CH5, and CH6, shown in Fig. 6, but it is in reasonable agreement considering the approximations used.

An examination is also made of another interesting phenomenon, *viz.*, variation of magnetization conductivity with temperature. This is illustrated in Fig. 11

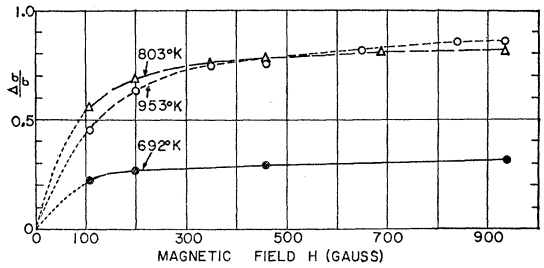

FIG. 11. Fractional change in conductivity for sample CH5 *versus* the magnetic field with temperature as a variable parameter. At 500°K no measurable change of conductivity with magnetic field (up to 1000 gauss) was observed.

for the case of CH5. The data are consistent with the model which has been proposed. As the temperature of the sample is lowered, the saturated value for the fractional change in conductivity decreases, indicating that at lower temperatures the mechanism of semiconduction, which is relatively unaffected by the magnetic field, becomes important.

The author expresses his appreciation to Dr. R. G. Breckenridge for his encouragement and suggestions throughout the course of this work. He also thanks Mr. W. B. Haliday and Mr. J. R. Nall for their valuable assistance in preparing the magnesium oxide crucibles and constructing most of the tubes. The author has benefited from discussions with many people and is especially indebted to Dr. C. H. Page, Dr. W. Gruner, Dr. M. Abramowitz, Dr. G. F. Rouse, and Dr. F. G. Brickwedde.